Int J Clin Exp Pathol 2016;9(12):12399-12406
www.ijcep.com /ISSN:1936-2625/IJCEP0028965

Original Article

Construction of HSP27-expressing lentiviral vector and interaction with contraction-associated proteins in the infection model with cells

Yunfeng Jiang, Chao Yan, Yuhui Wang, Congbin Peng, Huadong Zhu, Cheng Zhou, Guozheng Li

Department of Anesthesiology, Tongde Hospital of Zhejiang Province, Hangzhou 310012, Zhejiang, China

Received March 23, 2016; Accepted May 28, 2016; Epub December 1, 2016; Published December 15, 2016

Abstract: Objective: We investigated the proper method of constructing HSP27-expressing lentiviral vector and its effect on contraction-related proteins in the infection model in rat detrusor smooth muscle cells (DSMCs). Method: Using LV5 shuttle plasmid, cloning was performed at two restriction sites, NotI and BamHI. LV5-3G-HSP27 (invalid phosphorylated mutant) and LV5-3D-HSP27 (valid phosphorylated mutant) lentiviral vectors were cloned. The recombinant vectors were verified by restriction enzyme digestion and sequenced. The two verified vectors were further packaged and purified, and used to infect the rat DSMCs. In the meantime, the binding capacity of phosphorylated HSP27 to caldesmon (CaD) and tropomyosin (TM) was analyzed by co-immunoprecipitation assay. Result: Green fluorescent particles were seen in the cells infected by LV5-3G-HSP27 and LV5-3D-HSP27 lentiviral vectors, indicating that the cells were successfully infected. Co-immunoprecipitation assay showed that the phosphorylated HSP27 bound to CaD, but not to TM. Conclusion: We successfully built the lentiviral vector expressing phosphorylated HSP27, which was packaged and purified to obtain the infectious viral particles. The cells were infected by the lentiviral vector and the binding capacity of the phosphorylated HSP27 to contraction-related proteins was analyzed.

Keywords: HSP27, lentiviral vector, detrusor smooth muscle cells, CaD, TM

Introduction

Heat shock protein 27 (HSP27), named according to its molecular weight, is an important protein involved in drug resistance, cell growth and apoptosis, tumor occurrence and metastasis [1, 2]. Its functions may be related to covalent modification of the protein. Under normal conditions, HSP27 is lowly expressed and exists as polymer, which is usually inactive. But under stressful conditions, HSP27 is highly expressed with a higher phosphorylation level, making HSP27 active for fulfilling its functions [3]. HSP27 has three phosphorylation sites, serine-15, -78 and -82. After phosphorylation, the polymer will become smaller tetramer, which is the active form [4].

The normal functioning of bladder largely depends on the contractility of DSMCs, which is in turn controlled by the integrity of actin skeleton. Therefore, stabilizing myofilament structure is the guarantee for normal contraction of DSMCs. Various mechanisms can impair the contraction of DSMCs by affecting the myofilaments [5, 6]. In this study, we built the lentiviral vector expressing phosphorylated HSP27 and studied its binding capacity to contraction-related proteins. We hope to provide new insights into the treatment of bladder dysfunction.

Materials and methods

Construction of LV5-3G-HSP27 lentiviral vector

DNA endonuclease and DNA ligase were purchased from Fermentas (USA). DNA gel extraction kit was purchased from Beijing Tiangen Biotechemical Technology Co., Ltd. The primers were synthesized by Western Technology. First 3G-HSP27 fragment was obtained by PCR amplification. To the upstream and downstream primers of the target gene the homologous sequences flanking NotI and BamHI on the LV5

Table 1. Primers for the amplification of 3G-HSP27

B2023-1	AGGGTTCCAAGCTTAAGCGG
B2023-2	GGCGCTCGGTCATGGTGGCGCGGCCGCTTAAGCTTGGAACCC
B2023-3	ACCATGACCGAGCGCCGCGTGCCCTTCTCGCTACTGCGGAGC
B2023-4	AGTCCCGGAACGGCTCCCAGCCGGGGCTCCGCAGTAGCGAGA
B2023-5	GAGCCGTTCCGGGACTGGTACCCTGCCCACAGCCGCCTCTTC
B2023-6	AACCGAGGCACCCCGAAAGCTTGATCGAAGAGGCGGCTGTGG
B2023-7	CGGGGTGCCTCGGTTTCCCGATGAGTGGTCTCAGTGGTTCAG
B2023-8	ATAGCCGGGCCAACCAGCGGAGCTGAACCACTGAGACCACTC
B2023-9	CTGGTTGGCCCGGCTATGTGCGCCCTCTGCCCGCCGCGACCG
B2023-10	GGCCAGGGTCACTGCTGCGGGGCCCTCGGCGGTCGCGGCGGG
B2023-11	AGCAGTGACCCTGGCCAGGCCCGCCTTCGGCCGGGCGCTCAA
B2023-12	CTCTGAGACACCGCTGCTGAGTTGCCGGTTGAGCGCCCGGCC
B2023-13	AGCAGCGGTGTCTCAGAGATCCGACAGACGGCCGATCGCTGG
B2023-14	GAAGTGGTTGACGTCCAGGGACACGCGCCAGCGATCGGCCGT
B2023-15	CCTGGACGTCAACCACTTCGCTCCTGAGGAGCTCACAGTTAA
B2023-16	TCCACCACGCCTTCCTTGGTCTTAACTGTGAGCTCCTCAGGA
B2023-17	AAGGAAGGCGTGGTGGAGATCACTGGCAAGCACGAAGAAAGG
B2023-18	GAGATGTAGCCATGTTCATCCTGCCTTTCTTCGTGCTTGCCA
B2023-19	AGGATGAACATGGCTACATCTCTCGGTGCTTCACCCGGAAAT
B2023-20	GGTCCACACCTGGAGGGAGCGTGTATTTCCGGGTGAAGCACC
B2023-21	CCCTCCAGGTGTGGACCCCACCCTGGTGTCCTCTTCCCTGTC
B2023-22	CCACGGTGAGTGTGCCCTCAGGGGACAGGGAAGAGGACACCA
B2023-23	GGCACACTCACCGTGGAGGCTCCGCTGCCCAAAGCAGTCACA
B2023-24	CGGAATGGTGATCTCCGCTGATTGTGTGACTGCTTTGGGCAG
B2023-25	GCGGAGATCACCATTCCGGTCACTTTCGAGGCCCGTGCCCAA
B2023-26	AGACTGTTCCGACTCTGGGCCTCCAATTTGGGCACGGGCCTC
B2023-27	CCCAGAGTCGGAACAGTCTGGAGCCAAGTAGGGATCCGACAC
B2023-28	ATCAGTAGAGAGTGTCGGATCCCTACTTGG
B1866-1	AGCAGTGACCCTGGCCAGGCCCGCCTTCGGCCGGGC
B1866-70	CGGAATGGTGATCTCCGCTGATTGTGTGACTGCTTTGG

plasmid were added, respectively, for subcloning of the vector. The primer sequences are shown in **Table 1**. The primers were dissolved to 50 μM and equal amounts of the primers were added to the same 1.5 ml centrifuge tube with proper mixing. Thus the mix (B2023-1 to B2023-28) was prepared. The first round of PCR was carried out using the mix under the following conditions: 95°C for 3 min, 95°C for 30 sec, 55°C for 3 sec, 72°C for 3 sec, 30 cycles, and final extension at 72°C for 5 min. The second round of PCR was carried out using B1866-1 and B1866-70, the template being the products of the first round of PCR. The same PCR system and conditions were used as above. After PCR, agarose electrophoresis was performed, and the gel was cut out to recover 3G-HSP27 fragment. The target gene was cloned to LV5 shuttle plasmid, which was digested with NotI and BamHI at 37°C for 2 h. The LV5 vector was recovered using DNA gel extraction kit. With ClonExpress® Entry One Step Cloning Kit, the amplified fragment was cloned to the linearized LV5 vector. The competent cells were prepared by calcium chloride method and transfected with the ligation product. The clones were picked from the plate, and Plasmid Mini Preparation Kit was used to identify the positive clones. The extracted plasmids were verified by double restriction enzyme digestion at 37°C. Electrophoresis was conducted 1 h later. The clones with a target band of desired size were the positive clones. After that, 200 ul of the positive clones was taken and sequenced. The sequences were aligned with those of the target genes. Glycerin bacterial LB medium was used to obtain sufficient recombinant plasmids for subsequent experiments.

Construction of LV5-3D-HSP27 overexpressing lentiviral vector

The 3D-HSP27 overexpressing lentiviral vector was constructed using the same method as above. The primers for the first round of PCR (B2022-1 to B2022-28) are shown in **Table 2**. The second round of PCR was performed using B1866-1 and B1866-70, the template being the products of the first round of PCR. Recombinant plasmid was extracted and verified by double restriction enzyme digestion and electrophoresis. The sequences were aligned and analyzed with those of the target gene.

Packaging and purification of LV5-3G-HSP27 and LV5-3D-HSP27 overexpressing lentiviral vectors

The lentiviral shuttle plasmids and the helper plasmids were prepared. The four plasmids were subjected to high-purity endotoxin-free extraction. The four-plasmid system was used, comprised of LV5 (shuttle plasmid), PG-p1-

Table 2. Primers for the amplification of 3D-HSP27

B2022-1	AGGGTTCCAAGCTTAAGCGGCCGCGC
B2022-2	AAGGGCACGCGGCGCTCGGTCATGGTGGCGCGGCCGCTTAAG
B2022-3	CGCCGCGTGCCCTTCTCGCTACTGCGGAGCCCCAGGTGGGAG
B2022-4	TGGGCAGGGTACCAGTCCCGGAACGGCTCCCACCTGGGGCTC
B2022-5	GACTGGTACCCTGCCCACAGCCGCCTCTTCGATCAAGCTTTC
B2022-6	CATCGGGAAACCGAGGCACCCCGAAAGCTTGATCGAAGAGGC
B2022-7	GCCTCGGTTTCCCGATGAGTGGTCTCAGTGGTTCAGCTCCGC
B2022-8	AGGGCGCACATAGCCGGGCCAACCAGCGGAGCTGAACCACTG
B2022-9	CGGCTATGTGCGCCCTCTGCCCGCCGCGACCGCCGAGGGCCC
B2022-10	GGCGGGCCTGGCCAGGGTCACTGCTGCGGGGCCCTCGGCGGT
B2022-11	GGCCAGGCCCGCCTTCAGGCGGGCGCTCAACCGGCAACTCAG
B2022-12	TGTCGGATCTCTGAGACACCGCTGCTGAGTTGCCGGTTGAGC
B2022-13	GGTGTCTCAGAGATCCGACAGACGGCCGATCGCTGGCGCGTG
B2022-14	AGGAGCGAAGTGGTTGACGTCCAGGGACACGCGCCAGCGATC
B2022-15	GTCAACCACTTCGCTCCTGAGGAGCTCACAGTTAAGACCAAG
B2022-16	GTGATCTCCACCACGCCTTCCTTGGTCTTAACTGTGAGCTCC
B2022-17	AGGCGTGGTGGAGATCACTGGCAAGCACGAAGAAAGGCAGGA
B2022-18	CACCGAGAGATGTAGCCATGTTCATCCTGCCTTTCTTCGTGC
B2022-19	CATGGCTACATCTCTCGGTGCTTCACCCGGAAATACACGCTC
B2022-20	AGGGTGGGGTCCACACCTGGAGGGAGCGTGTATTTCCGGGTG
B2022-21	GTGTGGACCCCACCCTGGTGTCCTCTTCCCTGTCCCCTGAGG
B2022-22	GCGGAGCCTCCACGGTGAGTGTGCCCTCAGGGGACAGGGAAG
B2022-23	CCGTGGAGGCTCCGCTGCCCAAAGCAGTCACACAATCAGCGG
B2022-24	GAAAGTGACCGGAATGGTGATCTCCGCTGATTGTGTGACTGC
B2022-25	ATCACCATTCCGGTCACTTTCGAGGCCCGTGCCCAAATTGGA
B2022-26	TCCAGACTGTTCCGACTCTGGGCCTCCAATTTGGGCACGGGC
B2022-27	AGAGTCGGAACAGTCTGGAGCCAAGTAGGGATCCGACACTCT
B2022-28	ATCAGTAGAGAGTGTCGGATCCCTACTT

VSVG, PG-P2-REV and PG-P3-RRE. LV5 expressed green fluorescent protein (GFP); PG-p1-VSVG, PG-P2-REV and PG-P3-RRE contained the components needed for viral packaging. The 293T cells were used as the host cells and cultured in the 10 cm culture dish until reaching 80-90% confluence, and then they were inoculated to a 15 cm culture dish. DMEM containing 10% FBS was added and the cells were placed into a 37°C 5% CO_2 incubator overnight. For plasmid transfection, 1.5 ml serum-free DMEM was added into a sterile 5 ml centrifuge tube. Then shuttle plasmid and helper plasmid containing 3G-HSP27 and 3D-HSP27 sequences (pGag/Pol, pRev and pVSV-G) were added and mixed well. Another sterile 5 ml centrifuge tube was added with 1.5 ml of serum-free DMEM and 300 ul RNAi-Mate successively, mixed well and stood at room temperature for 5 min before combining the contents of the two tubes. Then the mixture stood at room temperature for 20-25 min and was added dropwise into a 15 cm culture dish and placed into a 37°C 5% CO_2 incubator for 4-6 h. The transfection fluid was discarded and DMEM containing 10% FBS was added. After that, the cells were further cultured in the 37°C 5% CO_2 incubator for 72 h.

The viral supernatant was collected and centrifuged at 4°C at 4000 g for 10 min. The supernatant was collected, filtered through a 0.45 μm sieve and subjected to ultraspeed centrifugation. The white precipitate at the bottom of the centrifuge tube was the viral particles, which were purified by density gradient centrifugation method using cesium chloride. Into the supernatant 50 ml of PEG8000 (20% PEG8000, 2.5 M Nacl) was added and the viral particles were precipitated on ice for 1 h. The precipitate was then suspended in 10 ml of 1.10 g/ml CsCl (20 mM Tris-Hcl as solvent, pH 8.0) and centrifuged at 4°C at 7000 rpm for 5 min. The viral suspension was collected. CsCl gradient solutions were prepared and added with 5 ml of viral suspension. This was followed by centrifugation at 20000 rpm at room temperature for 2 h. The viral layer with a density of 1.30-1.40 g/ml was collected into the dialysis bag and viral titer was determined.

Detection of viral titer: The 293T cells were inoculated to a 96-well plate at the density of 3×10^4 cells per well and cultured at 37°C in a 5% CO_2 incubator for 24 h. The viral particles (10 ul) were diluted into 4 gradients using DMEM containing 10% FBS. Into each well 100 μl of diluted viral particles was added and the blank control group was set up. The cells were cultured at 37°C in a 5% CO_2 incubator for 24 h. The fluorescent cells were counted under the fluorescence microscope and viral titer was calculated based on the times of dilution. Viral titer (BT = TU/ml, transducing units) was calculated as follows: TU/μl = (P × N/100 × V) × 1/

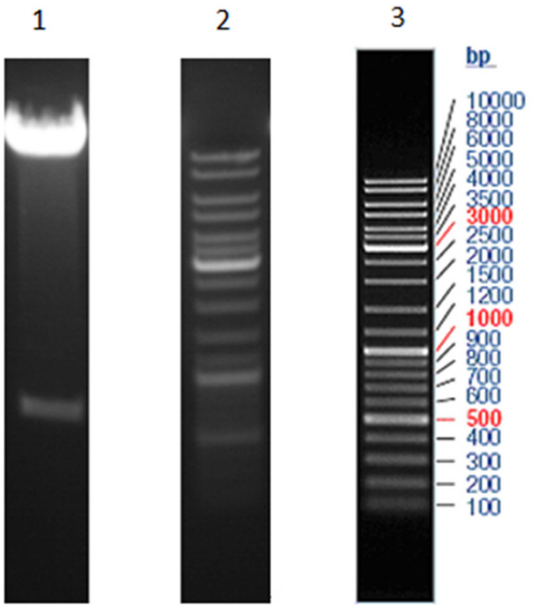

Figure 1. Double restriction enzyme digestion and electrophoresis. Channel 1: Double restriction enzyme digestion of LV5-3G-HSP27 recombinant plasmid (V7931-1) by NotI and BamHI; Channel 2: marker (Fermentas SM0331); Channel 3: marker (Fermentas SM0331).

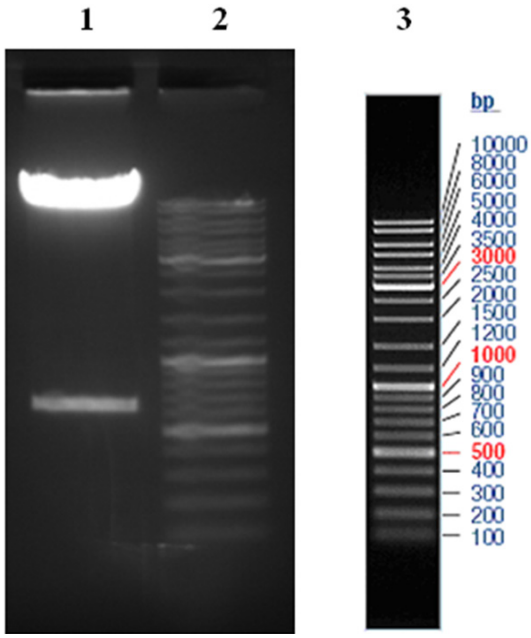

Figure 2. Double restriction enzyme digestion and electrophoresis. Channel 1: Double restriction enzyme digestion of LV5-3D-HSP27 recombinant plasmid (V7931-1) by NotI and BamHI; Channel 2: marker (Fermentas SM0331); Channel 3: marker (Fermentas SM0331).

DF, P = % GFP + cells, N = number of cells during transfection, V = volume of diluted viral particles added into each well (μl), DF = dilution factor = 1 (undiluted), 10-1 (diluted 1/10) and 10-2 (diluted 1/100).

Transfection of DSMCs with LV5-3G-HSP27 and LV5-3D-HSP27 vectors

Rat DSMCs obtained from primary culture were used and transfected with the constructed lentiviral vectors. Three groups were set up, LV5-3G-HSP27 homo (titer $1*10^8$ TU/mL), LV5-3D-HSP27 homo (titer $1*10^8$ TU/mL) and LV5 NC (negative control) (titer $5*10^8$ TU/mL). Log phase DSMCs were harvested and resuspended in serum-free culture medium, with the cell density adjusted to 2×10^6/ml. The cells were inoculated to a 24-well plate at the density of 5×10^4 cells per well. The volume of culture medium added into each well was 250 μl. Transfection was conducted when the cells grew to about 70% confluence.

Viral particles were prepared the next day. The lentiviral vectors were taken out from 4°C, centrifuged for 20 s and diluted by adding the culture medium based on MOI. To ensure optimal transfection efficiency, minimum amount of the culture medium was added. The lentiviral vectors were added into the 24-well plate along with 5 ug/mL polybrene reagent. The cells were incubated at 37°C in a 5% CO_2 incubator overnight. The culture medium was replaced on the third day. After 24 h, the culture medium containing the lentiviral vectors was replaced by normal culture medium at 500 ul per well. Transfection efficiency was determined on the sixth day. The fluorescent cells were observed under the inverted fluorescence microscope.

Determination of binding capacity of phosphorylated HSP27 to CaD and TM by co-immunoprecipitation assay

The binding capacity of the phosphorylated HSP27 to CaD and TM was determined by co-immunoprecipitation assay. Six groups were set up: 1. Normal control group; 2. 3G-HSP27 overexpressing lentiviral vector group (invalid phosphorylated mutant); 3. 3D-HSP27 overexpressing lentiviral vector group (valid phosphorylated mutant); 4. Normal control + 0.1 uM acetylcholine group; 5. 3G-HSP27 overexpressing lentiviral vector + 0.1 uM acetylcholine group;

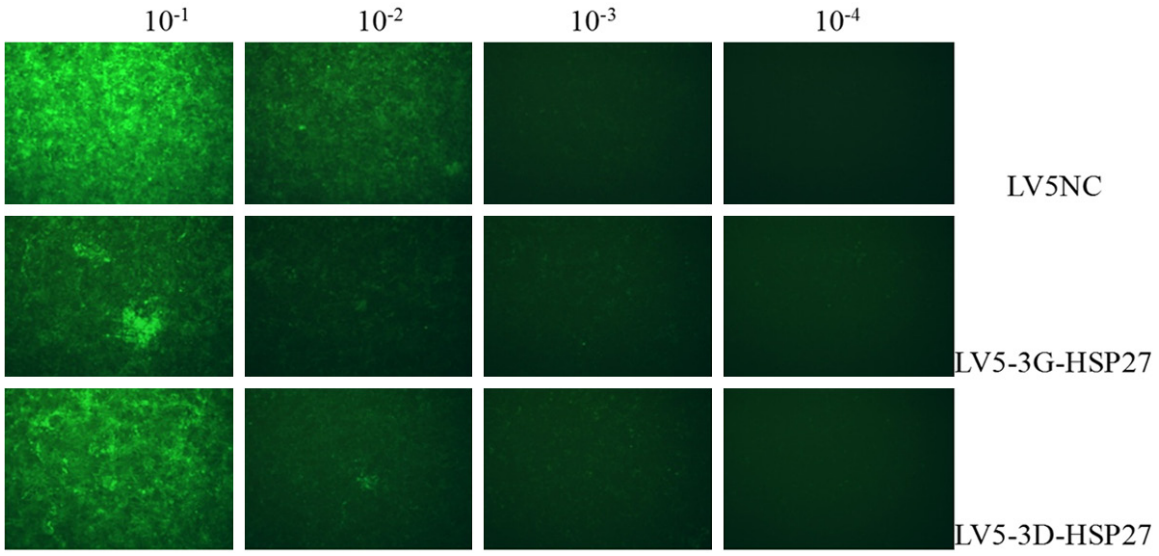

Figure 3. Packaging and purification of LV5-3G-HSP27 and LV5-3D-HSP27 lentiviral vectors.

6. 3D-HSP27 overexpressing lentiviral vector + 0.1 uM acetylcholine group. The purified CaD and TM antibodies were immobilized to the surface of cured resin. The protein complexes were separated from the lysate of rat DSMCs. All lysates were passed through the resin column and eluted. The eluted proteins were analyzed by SDS-PAGE and WB so as to determine the binding capacity of phosphorylated HSP27 to CaD and TM.

Result

Construction of 3G-HSP27 overexpressing lentiviral vector

The LV5-3G-HSP27 lentiviral vector was verified by double restriction enzyme digestion and electrophoresis. The target bands of the clones were very clear (**Figure 1**). Moreover, as shown by DNA sequence alignment, the vector was successfully constructed.

Construction of 3D-HSP27 overexpressing lentiviral vector

After double restriction enzyme digestion and electrophoresis of the LV5-3D-HSP27 lentiviral vector, the target bands of the clone were very clear (**Figure 2**). Combining with DNA sequence alignment, the vector was successfully constructed.

Packaging and purification of LV5-3G-HSP27 and LV5-3D-HSP27 lentiviral vectors

LV5-3G-HSP27 and LV5-3D-HSP27 lentiviral vectors were packaged and purified. Green fluorescent particles were seen in the cells under the fluorescence microscope (**Figure 3**). At 72 h after transfection, the viral titer was 5×10^8 TU/ml in LV5 control group and 1×10^8 TU/ml in LV5-3G-HSP27 and LV5-3D-HSP27 vector group.

Lentiviral infection of DSMCs

After lentiviral infection, the DSMCs were observed under the fluorescence microscope. The cells in LV5 empty vector group, LV5-3G-HSP27 vector group and LV5-3D-HSP27 vector group all contained green fluorescent particles, indicating that the cells were successfully infected by the recombinant lentiviruses (**Figure 4A-C**).

Binding capacity of phosphorylated HSP27 to CaD and TM

The binding capacity of the phosphorylated HSP27 to CaD and TM was determined by co-immunoprecipitation assay. HSP27 maintained the binding capacity of CaD all the time no matter whether it was phosphorylated or not dephosphorylated and whether it was treated or not treated with acetylcholine. However, HSP27 did not bind to TM in any group (**Figure 5A** and **5B**).

Discussion

HSP27 is a heat shock protein discovered in human cells with molecular weight of 27 KDa. HSP27 gene contains the heat shock regulatory element and the stress regulatory element in

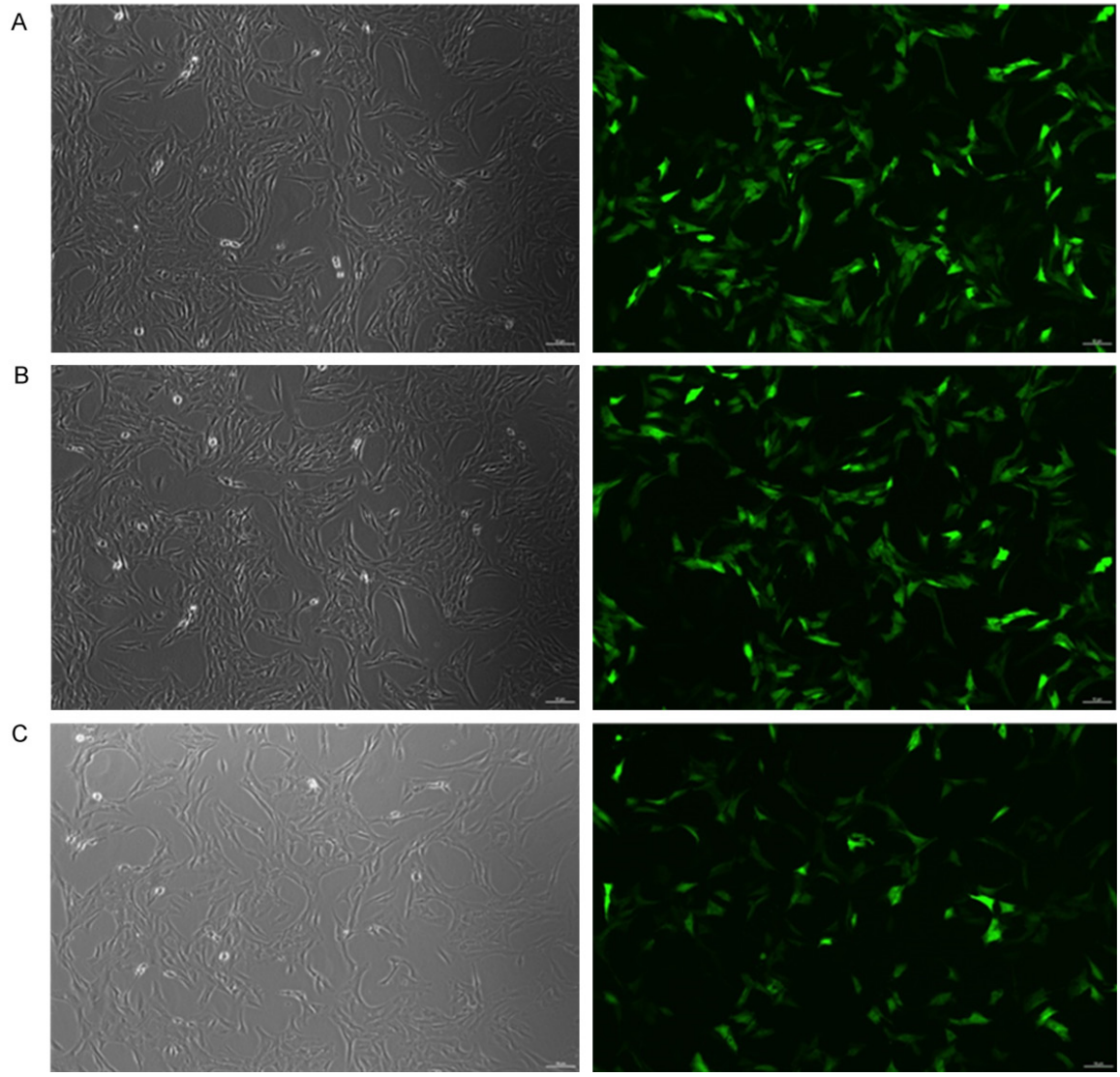

Figure 4. A. Infection by LV5 empty vector (100×); B. Infection by LV5-3G-HSP27 vector (100×); C. Infection by LV5-3D-HSP27 vector (100×).

the promoter region [7]. Its amino acid sequence has an N-terminal domain similar to that in crystal proteins. HSP27 shares many typical features of HSP subfamily, forming 400-800 KDa oligomers. The dissociation or polymerization of the oligomers depends on the biological functions to be achieved. For example, the oligomers are synthesized in order to regulate the intercellular active oxides and to maintain the glutathione level. The dissociation of oligomers is needed for it to act as the chaperone [8, 9]. The cellular defense affected by HSP27 may work through the following mechanism [10-16]. Firstly, the synthesis of HSP is inhibited so that the number of unfolded proteins in the eukaryotic cells decreases, thus reducing the damage to the cells. Secondly, HSP27 can prevent the damage of actin, maintain cytoskeleton stability and enhance thermal stability. Thirdly, HSP27 can facilitate RNA and protein synthesis after heat shock stress, thus assisting the repair of damage caused by heat shock stress before cell death. Fourthly, HSP27 helps maintain the glutathione level, reducing intercellular active oxides and cellular oxidation. Moreover, HSP27 is involved in the PKB-activated signaling pathway under stressful conditions, possibly regulating the cell apoptosis. According to the literature report, HSP27 inhibits cell apoptosis by inhibiting the activation of caspases [17]. In response to high heat and stimulation from cytochalasin, HSP27 is

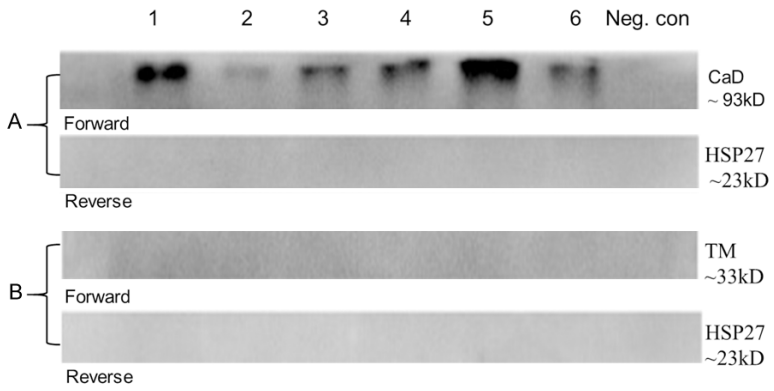

Figure 5. A. Binding capacity of CaD to phosphorylated HSP27; B. Binding capacity of TM to phosphorylated HSP27.

overexpressed to enhance the stability of F-actin filaments. Therefore, the damage of cytoskeleton is prevented, which is conducive to cell survival [18].

Contractile dysfunction of DSMCs is usually secondary to urinary tract obstruction, neurogenic bladder, diabetic bladder or the use of some drugs. Contractile dysfunction of DSMCs, a common disorder in clinical practice, is only poorly treated by various drugs [19]. Contraction of DSMCs is the most important function of bladder. The cytoskeleton or actin of DSMCs may be irreversibly damaged as a result of persistent urinary tract obstruction, neurologic diseases or chronic metabolic diseases. This will further contribute to irreversible impairment of bladder functions or even loss of contractility [20]. HSP27 is the chaperon responsible for maintaining cytoskeleton stability of various smooth muscle cells, including DSMCs. The expression and phosphorylation level of HSP27 may have changed in reduced contractility caused by lower urinary tract obstruction and show close connections with the degree of obstruction [21-23]. We found that the phosphorylated HSP27 bound to CaD but not to TM. So we believe HSP27 is an important protective factor in DSMCs, which regulates contractility by interacting with CaD. Following this idea, the contractile dysfunction of bladder can be treated by targeting at the expression or the phosphorylation level of HSP27.

Acknowledgements

This work was funded by the National Natural Sciences Fund (No. 81270845).

Disclosure of conflict of interest

None.

Address correspondence to: Yunfeng Jiang, Department of Anesthesiology, Tongde Hospital of Zhejiang Province, No.234 of Gucui Road, Xihu District, Hangzhou 310012, Zhejiang Province, China. Tel: +86-0571-89972000; Fax: +86-0571-89972000; E-mail: jiangyunfeng011@163.com

References

[1] Cumming KT, Paulsen G, Wernbom M, Ugelstad I, Raastad T. Acute response and subcellular movement of HSP27, alphaB-crystallin and HSP70 in human skeletal muscle after blood-flow-restricted low-load resistance exercise. Acta Physiol (Oxf) 2014; 211: 634-646.

[2] Hedges JC, Dechert MA, Yamboliev IA, Martin JL, Hickey E, Weber LA, Gerthoffer WT. A role for p38(MAPK)/HSP27 pathway in smooth muscle cell migration. J Biol Chem 1999; 274: 24211-24219.

[3] Ghosh A, Lai C, McDonald S, Suraweera N, Sengupta N, Propper D, Dorudi S, Silver A. HSP27 expression in primary colorectal cancers is dependent on mutation of KRAS and PI3K/AKT activation status and is independent of TP53. Exp Mol Pathol 2013; 94: 103-108.

[4] Korngut L, Ma CH, Martinez JA, Toth CC, Guo GF, Singh V, Woolf CJ, Zochodne DW. Overexpression of human HSP27 protects sensory neurons from diabetes. Neurobiol Dis 2012; 47: 436-443.

[5] Kirpatovsky VI, Plotnikov EY, Mudraya IS, Golovanov SA, Drozhzheva VV, Khromov RA, Chernikov DY, Skulachev VP, Zorov DB. Role of oxidative stress and mitochondria in onset of urinary bladder dysfunction under acute urine retention. Biochemistry (Mosc) 2013; 78: 542-548.

[6] Song B. [The role of bladder original excitation dysfunction in overactive bladder]. Zhonghua Yi Xue Za Zhi 2013; 93: 3329-3330.

[7] Li R, Li J, Sang D, Lan Q. Phosphorylation of AKT induced by phosphorylated Hsp27 confers the apoptosis-resistance in t-AUCB-treated glioblastoma cells in vitro. J Neurooncol 2015; 121: 83-89.

[8] Musiani D, Konda JD, Pavan S, Torchiaro E, Sassi F, Noghero A, Erriquez J, Perera T, Olivero M, Di Renzo MF. Heat-shock protein 27 (HSP27, HSPB1) is up-regulated by MET kinase inhibitors and confers resistance to MET-targeted therapy. FASEB J 2014; 28: 4055-4067.

[9] Nahomi RB, Palmer A, Green KM, Fort PE, Nagaraj RH. Pro-inflammatory cytokines downregulate Hsp27 and cause apoptosis of human retinal capillary endothelial cells. Biochim Biophys Acta 2014; 1842: 164-174.
[10] Oberbach A, Jehmlich N, Schlichting N, Heinrich M, Lehmann S, Wirth H, Till H, Stolzenburg JU, Volker U, Adams V, Neuhaus J. Molecular fingerprint of high fat diet induced urinary bladder metabolic dysfunction in a rat model. PLoS One 2013; 8: e66636.
[11] Pavan S, Musiani D, Torchiaro E, Migliardi G, Gai M, Di Cunto F, Erriquez J, Olivero M, Di Renzo MF. HSP27 is required for invasion and metastasis triggered by hepatocyte growth factor. Int J Cancer 2014; 134: 1289-1299.
[12] Tokuda H, Kato K, Kasahara S, Matsushima-Nishiwaki R, Mizuno T, Sakakibara S, Kozawa O. Significant correlation between the acceleration of platelet aggregation and phosphorylation of HSP27 at Ser-78 in diabetic patients. Int J Mol Med 2012; 30: 1387-1395.
[13] Qi S, Xin Y, Qi Z, Xu Y, Diao Y, Lan L, Luo L, Yin Z. HSP27 phosphorylation modulates TRAIL-induced activation of Src-Akt/ERK signaling through interaction with beta-arrestin2. Cell Signal 2014; 26: 594-602.
[14] Riazantseva NV, Kaigorodova EV, Maroshkina AN, Belkina MV, Novitskii VV. [Apoptosis-modulating effects of heat shock proteins: the influence of Hsp27 chaperone on TBA Bcl-2 family proteins in Jurkat cell line]. Vopr Onkol 2012; 58: 541-544.
[15] Lelj-Garolla B, Mauk AG. Roles of the N- and C-terminal sequences in Hsp27 self-association and chaperone activity. Protein Sci 2012; 21: 122-133.
[16] Wang X, Chen M, Zhou J, Zhang X. HSP27, 70 and 90, anti-apoptotic proteins, in clinical cancer therapy (Review). Int J Oncol 2014; 45: 18-30.
[17] Sun HB, Ren X, Liu J, Guo XW, Jiang XP, Zhang DX, Huang YS, Zhang JP. HSP27 phosphorylation protects against endothelial barrier dysfunction under burn serum challenge. Biochem Biophys Res Commun 2015; 463: 377-383.
[18] Zahari MS, Wu X, Pinto SM, Nirujogi RS, Kim MS, Fetics B, Philip M, Barnes SR, Godfrey B, Gabrielson E, Nevo E, Pandey A. Phosphoproteomic profiling of tumor tissues identifies HSP27 Ser82 phosphorylation as a robust marker of early ischemia. Sci Rep 2015; 5: 13660.
[19] Yoshimura N, Miyazato M, Kitta T, Yoshikawa S. Central nervous targets for the treatment of bladder dysfunction. Neurourol Urodyn 2014; 33: 59-66.
[20] Wolfe-Christensen C, Manolis A, Guy WC, Kovacevic N, Zoubi N, El-Baba M, Kovacevic LG, Lakshmanan Y. Bladder and bowel dysfunction: evidence for multidisciplinary care. J Urol 2013; 190: 1864-1868.
[21] Puri BK, Shah M, Julu PO, Kingston MC, Monro JA. Urinary bladder detrusor dysfunction symptoms in lyme disease. Int Neurourol J 2013; 17: 127-129.
[22] Ruan J, Qi Z, Shen L, Jiang Y, Xu Y, Lan L, Luo L, Yin Z. Crosstalk between JNK and NF-kappaB signaling pathways via HSP27 phosphorylation in HepG2 cells. Biochem Biophys Res Commun 2015; 456: 122-128.
[23] Stetler RA, Gao Y, Zhang L, Weng Z, Zhang F, Hu X, Wang S, Vosler P, Cao G, Sun D, Graham SH, Chen J. Phosphorylation of HSP27 by protein kinase D is essential for mediating neuroprotection against ischemic neuronal injury. J Neurosci 2012; 32: 2667-2682.